



Supplementary Information for

Study of protein folding under native conditions by rapidly switching the hydrostatic pressure inside an NMR sample cell

Cyril Charlier, T. Reid Alderson, Joseph M. Courtney, Jinfa Ying, Philip Anfinrud,* and Adriaan Bax*

* To whom correspondence should be addressed. E-mail: philip.anfinrud@nih.gov; bax@nih.gov

This PDF file includes:

Supplementary text
Figs. S1 to S7
Tables S1 to S4
References for SI reference citations

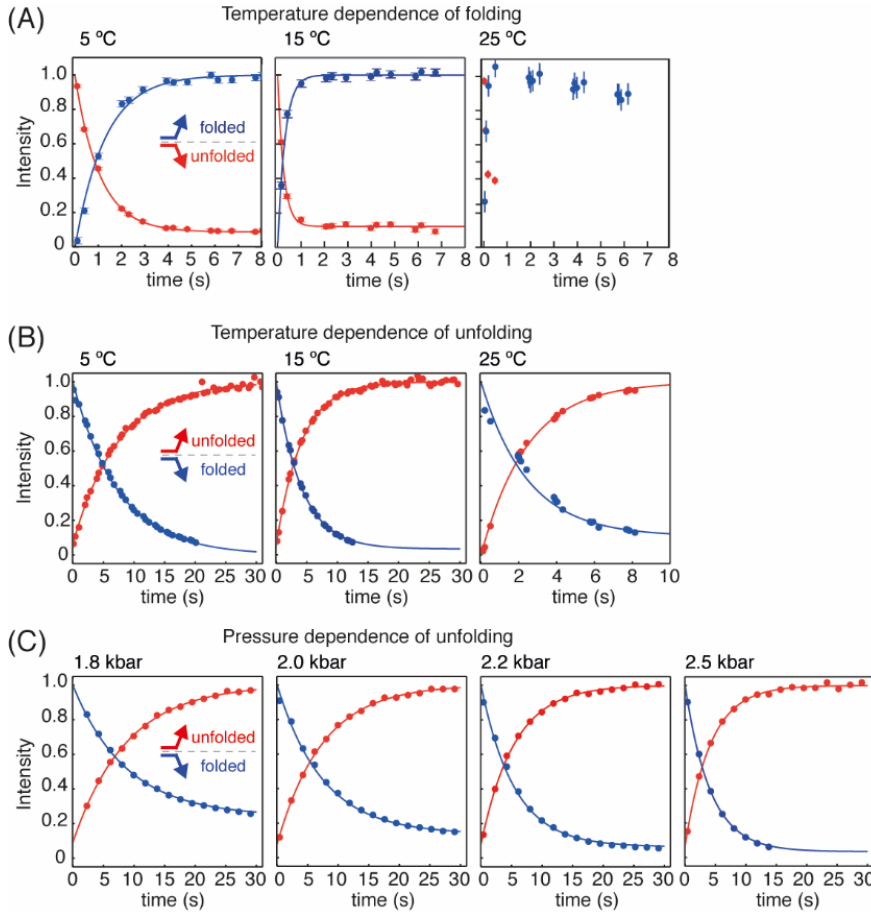


Fig. S1. Time dependence of the averaged NMR intensity of a set of representative well-resolved resonances in the HSQC spectra recorded at different temperatures and pressures with the scheme of Fig. 2A. (A) Intensities recorded for the folded and unfolded species as a function of time after the pressure drop from 2.5 kbar to 1 bar, at three different temperatures. Intensities at 25 °C are more sensitive to changes in line shape after a pressure jump, and folding rates were too fast to be fitted adequately with the scheme of Fig. 2A. Instead, they required the experiment of Fig. 3 to measure the kinetics of the folding process. (B) Intensities recorded for the folded and unfolded species as a function of time after the pressure is jumped from 1 bar to 2.5 kbar, at three different temperatures. (C) Kinetics of unfolding after the sample pressure is switched from 1 bar to the pressure indicated in the panel at 15 °C. Fitted rate constants are shown in Figure 4.

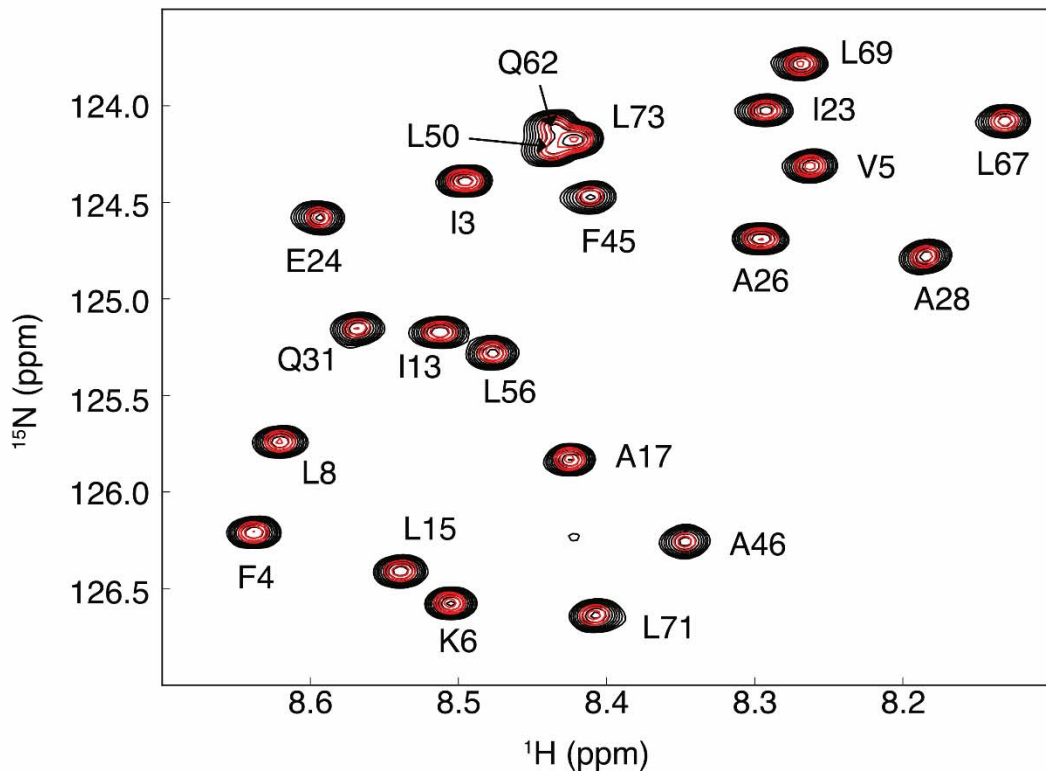


Fig. S2. Superposition of an expanded region of the 800 MHz ^1H - ^{15}N HSQC spectra of V17A/V26A ubiquitin, recorded at 15 °C, 25 mM sodium phosphate, pH 6.4, 2.5 kbar pressure, at sample concentrations of 50 μM (black) and 2 μM (red). Indistinguishable resonance positions and uniformly (25-fold) weaker intensities at 2 *versus* 50 μM confirm the absence of interprotein interactions.

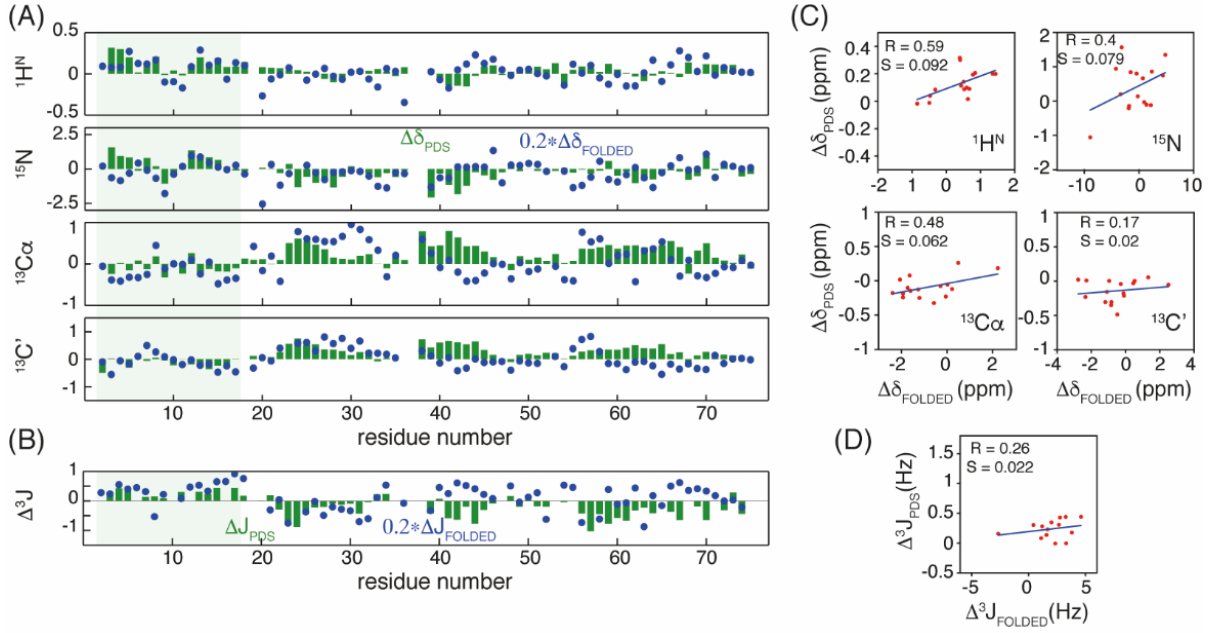


Fig. S3. Deviations of ubiquitin chemical shifts and $^3J_{\text{HNH}\alpha}$ couplings from random coil values. (A) Deviations of ubiquitin chemical shifts from random coil values for the pressure denatured state, $\Delta\delta_{\text{PDS}}$ (green bars), after applying the standard pressure corrections (1) for disordered polypeptides, and for the folded structure at 1 bar, $\Delta\delta_{\text{FOLDED}}$, scaled down five-fold (blue dots). Chemical shifts were measured on a sample of $700 \mu\text{M} ^{13}\text{C}/^{15}\text{N}/^2\text{H}$ V17A/V26A ubiquitin dissolved in 25 mM potassium phosphate buffer, pH 6.4, 25 °C, and ^2H isotope shift corrections (2) were applied to all values shown. Random coil chemical shift values, corrected for the effect of neighboring residues, pH, and temperature, were obtained from the POTENCI webserver (3). Note that increased dissociation of the phosphate buffer corresponds to a pH drop by ~0.9 units at 2.5 kbar relative to 1 bar, but effects of this pH drop on disordered chemical shifts as calculated by POTENCI are minimal. (B) Difference between $^3J_{\text{HN-H}\alpha}$ (in Hz) measured for wild type folded ubiquitin, and random coil values, ΔJ_{FOLDED} , scaled down five-fold (blue points) and between the pressure denatured state at 2.5 kbar of V17A/V26A ubiquitin and random coil values, Δ^3J_{PDS} (green bars). Random coil values are from (4). (C) Correlation between $\Delta\delta_{\text{PDS}}$ of residues 2 to 18 (after correction for the effect of pressure (1)) and $\Delta\delta_{\text{FOLDED}}$ for four types of backbone nuclei. The Pearson's correlation coefficient, R, and slope, S of a linear regression fit are marked in each panel. (D) Correlation between ΔJ_{PDS} and ΔJ_{FOLDED} for residues 2 to 18.

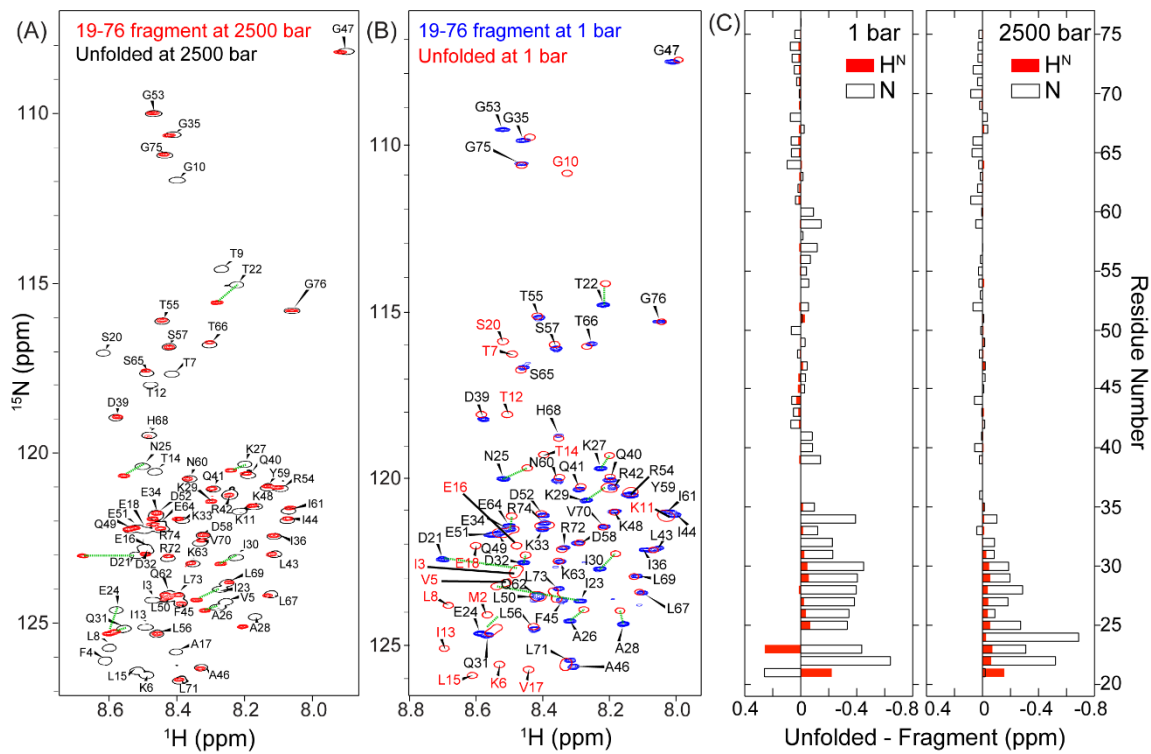


Fig. S4. Overlay of the unfolded ubiquitin NMR spectrum with that of the intrinsically unstructured ubiquitin peptide fragment P19-G76 (carrying the same V26A mutation as used for the full length protein). (A) Spectral overlay at 2.5 kbar, 19 °C. (B) Overlay of the experimental P19-G76 HSQC spectrum at 1 bar, with the synthetic full length ubiquitin spectrum, generated using the chemical shifts obtained with the pressure jump measurements of Figure 6, main text. (C) ^1H and ^{15}N chemical shift differences between full length unfolded ubiquitin and the P19-G76 fragment, at 1 bar (left) and 2.5 kbar (right).

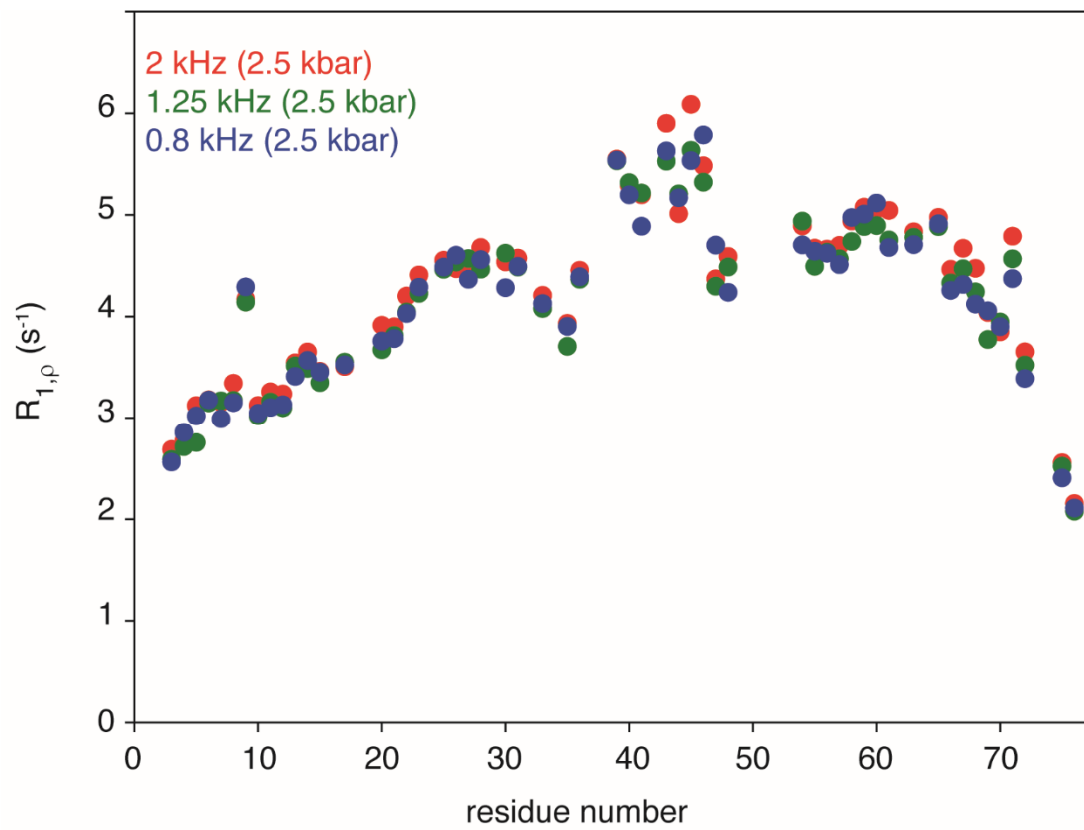


Fig. S5. ^{15}N transverse relaxation rates in the pressure-denatured state at 2.5 kbar, 22 °C. The same pulse scheme as used for the data of Fig. 7 was used, but at static high pressure. $^{15}\text{N} R_{1p}$ rates were measured at three strengths of the RF spin lock field, and corrected for offset and R_1 contributions.

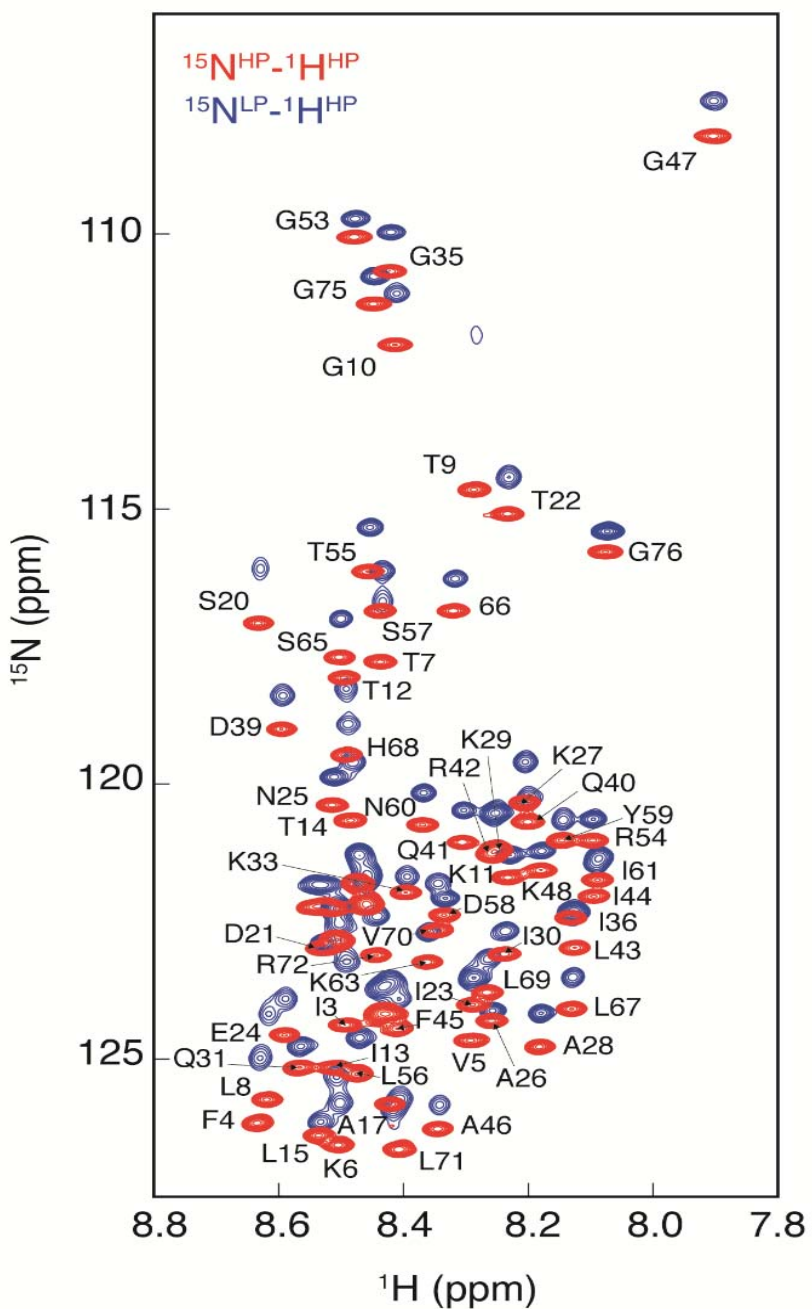


Fig. S6. Overlay of the static pressure 2D HSQC spectrum measured at 2.5 kbar (red) and the pressure-jump HSQC spectrum with ^{15}N evolution taking place at 1 bar, but ^1H detection at 2.5 kbar (blue). Spectra were recorded back-to-back for a sample containing 300 μM ubiquitin at 15 °C. Note that the ^{15}N shift evolution in the pressure jump spectrum takes place at 12 °C, and therefore includes a small effect (≤ 0.1 ppm) from the temperature dependence of the ^{15}N chemical shift.

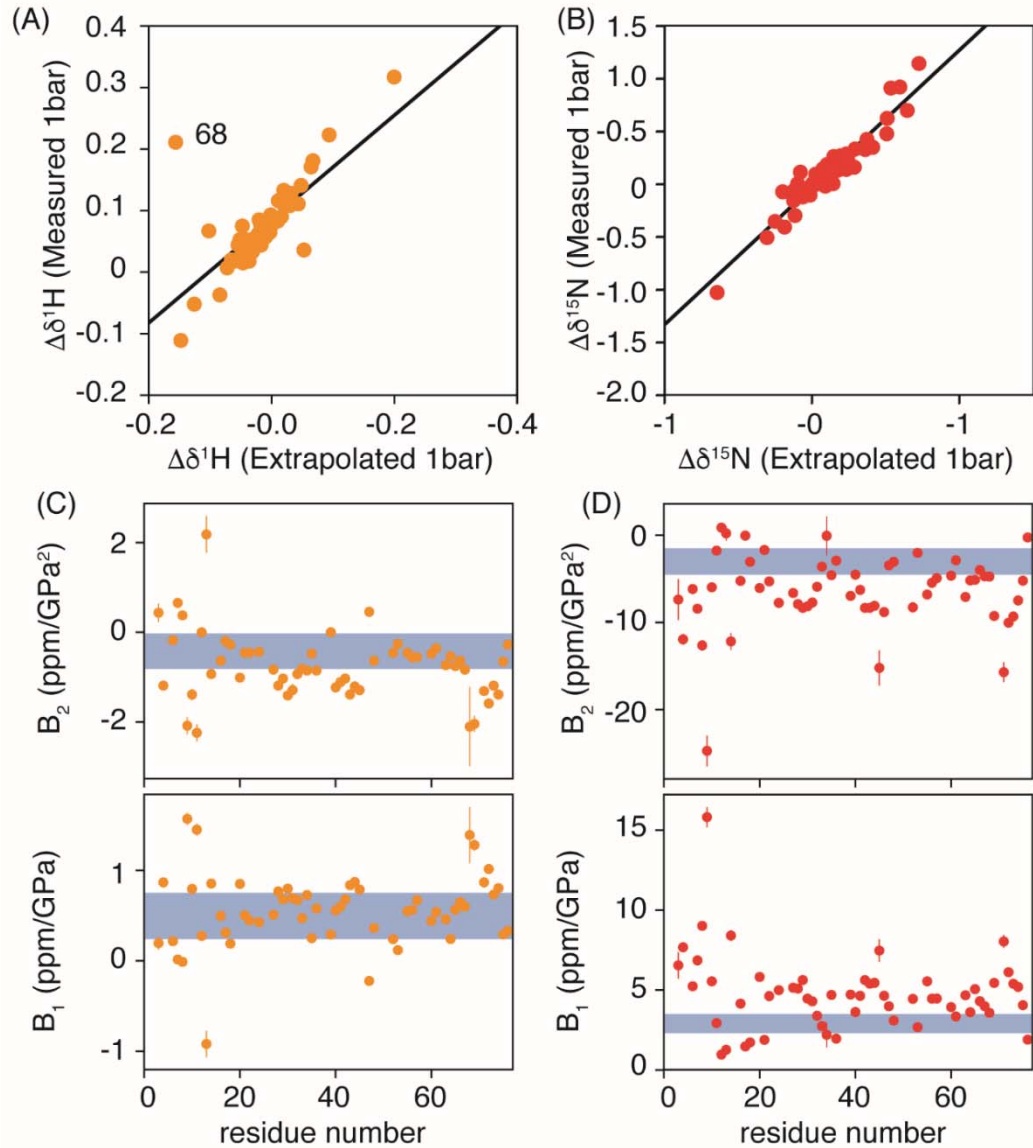


Fig. S7. Pressure dependence of ^1H and ^{15}N chemical shifts in the unfolded state. Chemical shifts are fitted to $\delta(p) = \delta(p_o) + B_1(p-p_o) + B_2(p-p_o)^2$, with $p_o = 1 \text{ bar} = 0.1 \text{ MPa}$. (A) Correlation between ^1H chemical shifts at 1 bar obtained from extrapolation of unfolded chemical shift values observed at pressures ranging from 1000-2500 bar, using a second order polynomial in the standard manner (5). The outlier corresponds to His-68, whose protonation state is pressure dependent. (B) Analogous correlation for unfolded ^{15}N shifts at 1 bar. (C) Best fitted B_1 and B_2 coefficients as a function of residue number for ^1H . (D) Best fitted B_1 and B_2 coefficients as a function of residue number for ^{15}N . The blue shaded regions correspond to the range observed in short linear peptides (6).

Table S1. Chemical shifts (in ppm) measured for the $^2\text{H}/^{15}\text{N}/^{13}\text{C}$ -enriched V17A/V26A ubiquitin double mutant at 25°C, pH 6.4 (at 1 bar).

Res	Folded (1 Bar)				Pressure Denatured States (2.5 kbar)				Unfolded (1 Bar)			
	HN	N	C α	C'	HN	N	C α	C'	HN	N	C α	C'
M1			54.01	170.56							54.72	172.79
Q2	8.88	122.65	55.11	174.99			55.23	175.09	8.66	123.9	55.39	175.15
I3	8.44	118.65	58.67	172.77	8.48	123.85	60.21	175.67	8.58	122.68	60.16	175.46
F4	8.62	119.88	55.10	175.06	8.61	125.57	57.05	175.40	8.66	124.45	57.01	175.79
V5	9.33	121.17	59.95	174.81	8.31	123.99	61.23	175.43	8.61	122.93	61.22	175.43
K6	9.01	127.67	54.24	177.14	8.50	126.00	55.87	176.75	8.63	125.38	55.61	177.2
T7	8.77	115.31	60.17	176.97	8.43	117.22	61.23	174.57	8.59	116.06	60.95	175.59
L8	9.15	121.26	57.11	178.90	8.61	125.31	54.99	177.72	8.78	123.61	55.87	178.28
T9	7.66	105.83	61.08	175.51	8.30	114.36	61.26	175.19		111.25	61.35	175.59
G10	7.86	109.20	44.93	173.97	8.42	111.68	45.03	174.03	8.43	110.65	45.16	174.3
K11	7.31	121.88	55.85	175.76	8.25	121.51	55.58	176.86	8.12	120.97	55.82	176.82
T12	8.66	120.43	61.96	174.34	8.49	117.62	61.66	174.44	8.61	117.9	62.09	174.71
I13	9.63	127.80	59.57	175.15	8.50	124.65	60.38	176.19	8.8	124.9	60.1	175.97
T14	8.76	120.86	61.60	173.54	8.48	120.04	61.18	174.20	8.5	119.1	60.89	174.38
L15	9.02	125.52	52.48	174.96	8.53	125.96	54.63	177.15	8.71	125.71	54.46	177.02
E16	8.05	121.42	54.21	175.04	8.52	122.38	55.73	175.95	8.58	121.83	55.78	176.15
A17	8.90	126.27	50.21	175.10	8.42	125.40	51.77	177.49	8.54	125.53	51.76	177.56
E18	8.82	119.66			8.51	121.92	53.79		8.66	121.83		
P19			64.94	175.54			62.92	177.25			63.19	177.47
S20	7.10	103.18	57.23	174.76	8.63	116.70	58.00	174.64	8.62	115.68	58.24	174.91
D21	8.06	123.73	55.07	176.11	8.55	122.64	54.02	176.50	8.58	122.5	54.39	176.84
T22	7.98	108.51	59.56	176.66	8.26	114.77	61.68	175.07	8.31	113.95	61.94	175.42
I23	8.50	121.14			8.29	123.62	61.22	176.94	8.36	123.05		
E24			60.16	179.10	8.60	124.23	56.65	176.98			57.19	177.39
N25	8.02	121.32	55.88	178.02	8.53	120.06	53.32	175.58	8.55	119.5	53.64	175.99
A26	8.17	123.13	55.35	179.30	8.30	124.06	52.79	178.42	8.38	123.74	53.23	178.79
K27	8.52	116.37	58.61	180.51	8.23	120.04	56.17	176.96	8.3	119.13	56.59	177.27
A28	8.05	123.97	54.84	180.40	8.20	124.43	52.24	177.99	8.27	123.77	52.57	178.28
K29	7.91	119.81	59.21	180.33	8.28	120.88	55.92	176.97	8.31	120.07	56.25	177.25
I30	8.22	121.48	65.52	178.20	8.25	122.72	60.71	176.48	8.28	122.07	61.13	176.78
Q31	8.58	123.33	59.47	178.82	8.58	124.72	55.42	175.86	8.64	124.27	55.74	176.11
D32	8.05	119.72	57.01	177.34	8.51	122.51	54.22	176.39	8.55	122.11	54.51	176.78
K33	7.45	115.35	57.74	177.84	8.41	121.66	56.00	176.82	8.48	121.21	56.39	177.12
E34	8.73	114.43	54.95	177.91	8.49	121.58	56.16	177.09	8.59	120.94	56.57	177.42
G35	8.56	108.84	45.59	173.90	8.44	110.38	44.96	173.85	8.54	109.58	45	174.09
I36	6.21	120.23			8.14	122.26	58.05		8.21	121.85		
P37												
P38			65.66	178.28			63.47	177.46			63.82	177.79
D39	8.55	113.50	55.42	177.06	8.59	118.62	54.45	176.88	8.68	117.9	54.87	177.34
Q40	7.87	116.88	55.17	175.35	8.23	120.33	55.96	176.73	8.3	119.78	56.29	177.08
Q41	7.52	118.02	56.13	176.15	8.33	120.74	56.37	176.62	8.39	120.06	56.54	176.92
R42	8.55	122.97	54.69	173.88	8.27	120.98	56.22	176.70	8.3	120.12	56.6	176.92
L43	8.80	124.10	52.71	175.33	8.15	122.69	55.14	177.56	8.17	121.95	55.42	177.8
I44	9.16	122.26	58.59	175.77	8.10	121.64	60.87	176.48	8.13	120.98	61.3	176.75
F45	8.85	124.65	56.05	174.69	8.41	124.03	57.31	175.72	8.46	123.43	57.63	175.98
A46	9.04	132.88	52.11	177.34	8.35	125.97	52.17	178.07	8.43	125.47	52.43	178.35
G47	8.15	102.42	44.89	173.71	7.94	108.00	45.11	174.22	8.09	107.26	45.16	174.44
K48	7.98	121.92	54.20	174.61	8.21	121.35	55.76	176.63	8.28	120.82	56.04	176.83
Q49	8.66	122.78	55.49	175.56	8.56	121.94	55.44	176.12	8.63	121.43	55.71	176.41
L50	8.57	125.49	53.93	176.71	8.45	123.95	54.88	177.63	8.51	123.38	54.98	178
E51	8.42	123.10	55.51	175.50	8.55	121.88	56.04	176.42	8.62	121.48	56.55	176.71
D52	8.19	120.32			8.48	121.47	54.11	177.06	8.5	120.87		
G53			44.75	174.85	8.49	109.81	45.44	174.73			45.4	175.07
R54	7.48	119.39	53.98	175.26	8.15	120.82	55.80	176.75	8.24	120.26	56.23	176.99
T55	8.85	108.69	59.51	176.47	8.46	115.85	61.54	174.83	8.52	114.93	61.8	175.19
L56	8.33	118.57	58.67	180.99	8.48	124.96	55.15	177.75	8.53	124.24	55.52	178.06
S57	8.77	113.28	60.70	178.31	8.44	116.61	58.24	174.59	8.46	115.78	58.66	174.88
D58	7.98	124.47	57.00	177.33	8.35	122.12	54.27	176.32	8.39	121.74	54.68	176.7
Y59	7.30	115.73	57.76	174.74	8.17	120.71	58.05	175.96	8.23	120.18	58.45	176.2
N60	8.22	115.63	53.87	174.16	8.40	120.48	53.15	175.40	8.45	119.79	53.54	175.73

I61	7.23	119.00	62.14	174.33	8.10	121.37	61.28	176.73	8.14	120.85	61.82	176.99
Q62	7.67	124.78	53.21	175.32	8.46	123.82	55.71	176.45	8.52	123.3	55.92	176.77
K63	8.43	119.99	57.59	176.13	8.39	122.95	56.32	177.07	8.45	122.29	56.63	177.36
E64	9.29	115.23	57.98	175.39	8.50	121.78	56.36	176.98	8.59	121.33	56.75	177.3
S65	7.91	115.60	60.72	172.01	8.52	117.28	58.36	175.39	8.57	116.54	58.64	175.68
T66	8.71	117.11	62.10	173.60	8.33	116.51	62.05	174.83	8.37	115.83	62.42	175.25
L67	9.50	127.73	53.48	175.22	8.17	123.93	55.28	177.33	8.21	123.22	55.8	177.65
H68	9.28	119.09	55.74	173.77	8.52	119.27	55.00	174.56	8.45	118.61	55.95	175.32
L69	8.29	123.57	53.40	175.44	8.28	123.58	55.08	177.33	8.23	122.75	55.5	177.66
V70	9.19	126.28	60.12	174.07	8.35	122.28	62.08	176.30	8.32	121.27	62.67	176.71
L71	8.13	122.85	53.67	177.86	8.41	126.31	54.87	177.32	8.43	125.28	55.23	177.72
R72	8.63	123.60	55.28	175.34	8.45	122.73	55.61	176.40	8.44	121.94	55.79	176.79
L73	8.38	124.38	54.42	177.45	8.42	123.89	54.81	177.60	8.47	123.18	54.96	177.92
R74	8.47	121.92	56.17	176.90	8.47	121.93	55.88	176.90	8.51	121.23	56.3	177.14
G75	8.51	111.00	44.80	173.63	8.46	110.99	45.01	173.88	8.56	110.41	45.07	173.99
G76	7.97	115.05	45.58		8.08	115.62	45.80		8.17	115.09		

Table S2. Time constants (in seconds) of folding and unfolding, derived from the temperature and pressure dependence of resonance intensities in the folded and unfolded states. For the joint analysis, the appearance of the folded state and disappearance of the unfolded state were fitted jointly.

Temperature dependence of folding (P = 2.5kbar)								
Observed state	5 °C			15 °C			25 °C	
Appearance of Folded state	1.3	+/-	0.1	0.31	+/-	0.03	0.15	+/- 0.01
Disappearance of Unfolded state	1.06	+/-	0.05	0.25	+/-	0.02	0.07	+/- 0.01
Temperature dependence of unfolding (P = 2.5kbar)								
Joint analysis	5 °C			15 °C			25 °C	
Joint analysis	7.5	+/-	0.1	4.1	+/-	0.1	2.5	+/- 0.1
Pressure dependence of unfolding (T = 15 °C)								
	1.8 kbar		2 kbar		2.2 kbar		2.5kbar	
Joint analysis	8.7	+/-	0.2	7.4	+/-	0.1	5.5	+/- 0.1
							4.1	+/- 0.1

Table S3. $^3J_{\text{HNH}\alpha}$ (Hz) of the pressure denatured state of the V17A/V26A double mutant of ubiquitin measured at 600 MHz, 2.5 kbar, 22 °C, pH 6.4 (at 1 bar). The $^3J_{\text{HNH}\alpha}$ random coil values shown in the second column were obtained from https://spin.niddk.nih.gov/bax/nmrserver/rc_3Jhnha/

Res	2.5 kbar <u>Shen et al.(4)</u>		2.5 kbar		1 Bar / 8 M Urea				2.5 kbar / 8 M Urea	
	$^3J_{\text{HnHa}}$	$^3J_{\text{HnHa}}$	$^3J_{\text{HnHa}}$	$^3J_{\text{HnHa}}$	$^3J_{\text{HnHa}}$	$^3J_{\text{HnHa}}$	$^3J_{\text{HnHa}}$	$^3J_{\text{HnHa}}$	$^3J_{\text{HnHa}}$	$^3J_{\text{HnHa}}$
M1	6.5									
Q2	6.8									
I3	7.5	7.8	+/-	0.1						
F4	7.1	7.5	+/-	0.1	6.9	+/-	0.3	6.9	+/-	0.2
V5	7.7	8.0	+/-	0.2	8.0	+/-	0.2	7.8	+/-	0.2
K6	6.5				6.8	+/-	0.1	6.4	+/-	0.1
T7	7.2	7.4	+/-	0.1	7.6	+/-	0.2	7.1	+/-	0.1
L8	6.5	6.7	+/-	0.2	7.9	+/-	0.1	7.5	+/-	0.1
T9	7.6	7.7	+/-	0.2	7.8	+/-	0.3	7.7	+/-	0.2
G10										
K11	6.4	6.7	+/-	0.1	6.6	+/-	0.1	6.4	+/-	0.1
T12	7.2	7.2	+/-	0.1	7.4	+/-	0.2	7.0	+/-	0.1
I13	7.3	7.6	+/-	0.1	8.1	+/-	0.1	7.5	+/-	0.1
T14	7.6	7.8	+/-	0.1	8.0	+/-	0.1	7.6	+/-	0.2
L15	6.5	7.0	+/-	0.1	7.2	+/-	0.2	6.8	+/-	0.2
E16	6.6	6.6	+/-	0.1	6.7	+/-	0.1	6.4	+/-	0.1
A17	5.4	5.8	+/-	0.1	5.8	+/-	0.1	5.5	+/-	0.1
E18	6.3	6.5	+/-	0.1	6.1	+/-	0.1	5.8	+/-	0.2
P19										
S20	6.4	6.4	+/-	0.1	6.7	+/-	0.1	6.4	+/-	0.1
D21	6.5	6.7	+/-	0.1	6.9	+/-	0.1	6.7	+/-	0.1
T22	7.4	7.1	+/-	0.1	7.5	+/-	0.1	7.4	+/-	0.1
I23	7.3	6.6	+/-	0.1	5.3	+/-	0.1	5.7	+/-	0.5
E24	6.5	5.6	+/-	0.1	6.0	+/-	0.1	5.8	+/-	0.2
N25	7.0	6.5	+/-	0.1	6.9	+/-	0.2	6.7	+/-	0.2
A26	5.3	5.1	+/-	0.1	6.7	+/-	0.3	5.2	+/-	0.2
K27	6.4	6.2	+/-	0.1				6.4	+/-	0.2
A28	5.2	5.1	+/-	0.1	5.2	+/-	0.1	4.8	+/-	0.2
K29	6.5	6.3	+/-	0.2	6.4	+/-	0.1	6.1	+/-	0.2
I30	7.0	6.9	+/-	0.2	7.3	+/-	0.1	6.9	+/-	0.2
Q31	7.0	6.6	+/-	0.2	6.9	+/-	0.1	6.6	+/-	0.2
D32	6.2	6.2	+/-	0.1	6.4	+/-	0.1	6.1	+/-	0.2
K33	6.4	6.7	+/-	0.1	6.8	+/-	0.1	6.5	+/-	0.2
E34	6.1	6.4	+/-	0.1	6.6	+/-	0.1	6.6	+/-	0.1
G35										
I36	7.5	7.5	+/-	0.1	7.6	+/-	0.1	7.2	+/-	0.1
P37										
P38										
D39	6.3	5.9	+/-	0.1	6.2	+/-	0.1	6.0	+/-	0.2
Q40	6.7	6.7	+/-	0.2				6.7	+/-	0.3
Q41	6.3	5.7	+/-	0.2	6.3	+/-	0.2	5.9	+/-	0.3
R42	6.5	5.9	+/-	0.2	6.6	+/-	0.2	6.1	+/-	0.3
L43	6.6	6.4	+/-	0.3				6.5	+/-	0.3
I44	8.0	7.2	+/-	0.2	8.0	+/-	0.1	7.6	+/-	0.1
F45	7.2	6.9	+/-	0.3	7.9	+/-	0.1	7.4	+/-	0.2
A46	6.0	5.9	+/-	0.3	5.4	+/-	0.5	5.8	+/-	0.4
G47										
K48	6.4	6.6	+/-	0.1	6.9	+/-	0.2	6.5	+/-	0.1
Q49	6.6	6.4	+/-	0.1	6.7	+/-	0.1	6.1	+/-	0.2
L50	6.3	6.3	+/-	0.1	6.6	+/-	0.1	6.2	+/-	0.2
E51	6.6	6.4	+/-	0.1	6.5	+/-	0.1	6.4	+/-	0.2
D52	6.5	6.3	+/-	0.1	6.5	+/-	0.1	6.4	+/-	0.1
G53										
R54	6.6	6.6	+/-	0.1	6.7	+/-	0.1	6.5	+/-	0.1
T55	7.3	7.3	+/-	0.1	7.6	+/-	0.1	7.2	+/-	0.2

L56	6.6	6.2	+/-	0.2	6.8	+/-	0.1	6.5	+/-	0.2
S57	6.9	5.9	+/-	0.3	6.6	+/-	0.1	6.4	+/-	0.2
D58	6.9	6.5	+/-	0.1	6.8	+/-	0.1	6.6	+/-	0.2
Y59	6.9	6.1	+/-	0.1	6.6	+/-	0.1	6.3	+/-	0.2
N60	7.6	7.0	+/-	0.2	7.4	+/-	0.2	7.1	+/-	0.3
I61	7.2	6.5	+/-	0.1	7.1	+/-	0.1	6.7	+/-	0.1
Q62	6.7	6.4	+/-	0.2	6.7	+/-	0.1	6.3	+/-	0.2
K63	6.2	5.9	+/-	0.2	6.2	+/-	0.1	6.1	+/-	0.2
E64	6.1	5.7	+/-	0.2	7.1	+/-	0.1	6.7	+/-	0.1
S65	6.3				6.3	+/-	0.3	6.0	+/-	0.4
T66	7.4	7.0	+/-	0.3	7.7	+/-	0.3	7.5	+/-	0.4
L67	6.6	6.0	+/-	0.2	6.3	+/-	0.1	6.1	+/-	0.2
H68	7.3							6.2	+/-	0.8
L69	6.5	6.3	+/-	0.2	7.1	+/-	0.1	6.8	+/-	0.1
V70	7.8	7.2	+/-	0.1	7.9	+/-	0.1	7.4	+/-	0.2
L71	6.4	6.4	+/-	0.2	7.0	+/-	0.1	6.6	+/-	0.2
R72	7.0	6.7	+/-	0.2	7.2	+/-	0.1	6.8	+/-	0.2
L73	6.3	6.6	+/-	0.1	7.0	+/-	0.1	6.5	+/-	0.1
R74	7.0	6.5	+/-	0.1	6.7	+/-	0.1			
G75										
G76										

Table S4. $R_1\rho$ values (s^{-1}) measured at spin lock-fields of 2 kHz, 1.25 kHz and 0.8 kHz, at indicated pressures of 1 bar and 2.5 kbar, after correction for the R_1 contribution and offset effects.

	2 kHz				1.25 kHz				0.8 kHz			
	1 bar		2.5 kbar		1 bar		2.5 kbar		1 bar		2.5 kbar	
M1												
Q2												
I3	6.4	+/- 0.1	2.7	+/- 0.04	7.2	+/- 0.1	2.6	+/- 0.03	8.8	+/- 0.1	2.6	+/- 0.03
F4	7.3	+/- 0.1	2.8	+/- 0.04	8.4	+/- 0.1	2.7	+/- 0.04	10.6	+/- 0.1	2.9	+/- 0.04
V5	7.9	+/- 0.1	3.1	+/- 0.04	8.9	+/- 0.1	2.8	+/- 0.04	11.9	+/- 0.1	3	+/- 0.04
K6	7.2	+/- 0.1	3.2	+/- 0.04	8	+/- 0.1	3.2	+/- 0.04	9.9	+/- 0.1	3.2	+/- 0.04
T7	7.8	+/- 0.1	3.2	+/- 0.04	8.8	+/- 0.1	3.2	+/- 0.04	10.9	+/- 0.1	3	+/- 0.04
L8	7.6	+/- 0.1	3.3	+/- 0.05	8.3	+/- 0.1	3.2	+/- 0.04	10.3	+/- 0.1	3.2	+/- 0.04
T9	17	+/- 0.3	4.2	+/- 0.05	19.2	+/- 0.3	4.1	+/- 0.04	25.3	+/- 0.4	4.3	+/- 0.05
G10	5.8	+/- 0.1	3.1	+/- 0.04	5.7	+/- 0.1	3	+/- 0.04	6.5	+/- 0.1	3.1	+/- 0.04
K11	5.4	+/- 0.1	3.3	+/- 0.04	5.4	+/- 0.1	3.2	+/- 0.04	5.6	+/- 0.1	3.1	+/- 0.04
T12	6.6	+/- 0.1	3.2	+/- 0.04	6.8	+/- 0.1	3.1	+/- 0.04	8.0	+/- 0.1	3.1	+/- 0.04
I13	6.9	+/- 0.1	3.6	+/- 0.04	7.9	+/- 0.1	3.5	+/- 0.04	8.9	+/- 0.1	3.4	+/- 0.04
T14	7.1	+/- 0.1	3.7	+/- 0.05	7.3	+/- 0.1	3.5	+/- 0.04	8.5	+/- 0.1	3.6	+/- 0.05
L15	5.9	+/- 0.1	3.5	+/- 0.04	5.9	+/- 0.1	3.4	+/- 0.04	6.9	+/- 0.1	3.5	+/- 0.04
E16												
A17	6.3	+/- 0.1	3.5	+/- 0.04	7	+/- 0.1	3.6	+/- 0.04	8.6	+/- 0.1	3.5	+/- 0.04
E18												
P19												
S20	10.3	+/- 0.1	3.9	+/- 0.04	13.8	+/- 0.2	3.7	+/- 0.04	18.4	+/- 0.3	3.8	+/- 0.04
D21	5.4	+/- 0.1	3.9	+/- 0.03	5.8	+/- 0.1	3.8	+/- 0.03	6.5	+/- 0.1	3.8	+/- 0.03
T22	6.3	+/- 0.1	4.2	+/- 0.04	7.4	+/- 0.1	4.1	+/- 0.04	9.3	+/- 0.1	4	+/- 0.04
I23	5.9	+/- 0.1	4.4	+/- 0.05	6.4	+/- 0.1	4.2	+/- 0.05	6.4	+/- 0.1	4.3	+/- 0.05
E24												
N25	7	+/- 0.1	4.6	+/- 0.05	5.7	+/- 0.1	4.5	+/- 0.04	6	+/- 0.1	4.5	+/- 0.05
A26	5.7	+/- 0.1	4.5	+/- 0.04	5.7	+/- 0.1	4.5	+/- 0.04	5.9	+/- 0.1	4.6	+/- 0.04
K27	6.2	+/- 0.1	4.4	+/- 0.05	6.6	+/- 0.1	4.6	+/- 0.04	7.7	+/- 0.1	4.4	+/- 0.04
A28	6.0	+/- 0.1	4.7	+/- 0.04	6.1	+/- 0.1	4.5	+/- 0.04	6.5	+/- 0.1	4.6	+/- 0.04
K29												
I30	6.1	+/- 0.1	4.5	+/- 0.05	6.5	+/- 0.1	4.6	+/- 0.05	6.9	+/- 0.1	4.3	+/- 0.05
Q31	6.1	+/- 0.1	4.6	+/- 0.06	6.5	+/- 0.1	4.5	+/- 0.05	6.7	+/- 0.1	4.5	+/- 0.05
D32												
K33	7	+/- 0.1	4.2	+/- 0.05	7.9	+/- 0.1	4.1	+/- 0.05	9.7	+/- 0.1	4.1	+/- 0.05
E34												
G35	4.9	+/- 0.1	3.9	+/- 0.05	4.7	+/- 0.1	3.7	+/- 0.04	5	+/- 0.1	3.9	+/- 0.05
I36	6.1	+/- 0.1	4.5	+/- 0.05	6.3	+/- 0.1	4.4	+/- 0.05	6.9	+/- 0.1	4.4	+/- 0.05
P37												
P38												
D39	7.5	+/- 0.1	5.6	+/- 0.05	8.9	+/- 0.1	5.5	+/- 0.05	11	+/- 0.1	5.5	+/- 0.05
Q40	7.2	+/- 0.1	5.3	+/- 0.07	7	+/- 0.1	5.3	+/- 0.06	8	+/- 0.1	5.2	+/- 0.07
Q41	6.4	+/- 0.1	5.2	+/- 0.06	6.7	+/- 0.1	5.2	+/- 0.06	7.2	+/- 0.1	4.9	+/- 0.06
R42												
L43	7.9	+/- 0.1	5.9	+/- 0.07	8.4	+/- 0.1	5.5	+/- 0.07	10.1	+/- 0.1	5.6	+/- 0.07
I44	7.4	+/- 0.1	5.0	+/- 0.06	7.7	+/- 0.1	5.2	+/- 0.06	8.4	+/- 0.1	5.2	+/- 0.06
F45	8.6	+/- 0.2	6.1	+/- 0.08	8.5	+/- 0.2	5.6	+/- 0.08	9.8	+/- 0.2	5.5	+/- 0.08
A46	8.0	+/- 0.1	5.5	+/- 0.06	9.5	+/- 0.1	5.3	+/- 0.06	10.5	+/- 0.1	5.8	+/- 0.06
G47	6.5	+/- 0.1	4.4	+/- 0.06	7.1	+/- 0.1	4.3	+/- 0.06	7.5	+/- 0.1	4.7	+/- 0.06
K48	5.8	+/- 0.1	4.6	+/- 0.05	6.1	+/- 0.1	4.5	+/- 0.05	6.3	+/- 0.1	4.2	+/- 0.05
Q49												
L50												

E51																				
D52																				
G53																				
R54	6.2	+/-	0.1	4.9	+/-	0.05	6.7	+/-	0.1	4.9	+/-	0.05	7	+/-	0.1	4.7	+/-	0.05		
T55	6.9	+/-	0.1	4.7	+/-	0.05	6.8	+/-	0.1	4.5	+/-	0.05	7.7	+/-	0.1	4.6	+/-	0.05		
L56	6.5	+/-	0.1	4.7	+/-	0.05	6.8	+/-	0.1	4.6	+/-	0.05	7.5	+/-	0.1	4.6	+/-	0.05		
S57	7.2	+/-	0.1	4.7	+/-	0.05	7.6	+/-	0.1	4.6	+/-	0.04	9.2	+/-	0.1	4.5	+/-	0.05		
D58	6.8	+/-	0.1	4.9	+/-	0.05	6.7	+/-	0.1	4.7	+/-	0.05	7.4	+/-	0.1	5	+/-	0.05		
Y59	7.5	+/-	0.1	5.1	+/-	0.05	8.5	+/-	0.1	4.9	+/-	0.05	10.1	+/-	0.1	5	+/-	0.05		
N60	7.3	+/-	0.1	5.1	+/-	0.06	7.6	+/-	0.1	4.9	+/-	0.05	8.3	+/-	0.1	5.1	+/-	0.05		
I61	7.2	+/-	0.1	5.1	+/-	0.05	7.3	+/-	0.1	4.8	+/-	0.05	7.8	+/-	0.1	4.7	+/-	0.05		
Q62																				
K63	7.3	+/-	0.1	4.8	+/-	0.05	7.8	+/-	0.1	4.8	+/-	0.05	9.2	+/-	0.1	4.7	+/-	0.05		
E64																				
S65	6.7	+/-	0.1	5	+/-	0.06	7.1	+/-	0.1	4.9	+/-	0.05	7.6	+/-	0.1	4.9	+/-	0.06		
T66	7.1	+/-	0.1	4.5	+/-	0.05	7.1	+/-	0.1	4.3	+/-	0.05	7.9	+/-	0.1	4.3	+/-	0.05		
L67	7.7	+/-	0.1	4.7	+/-	0.05	8.4	+/-	0.1	4.5	+/-	0.05	9.8	+/-	0.1	4.3	+/-	0.05		
H68	6.9	+/-	0.2	4.5	+/-	0.07	6.9	+/-	0.2	4.2	+/-	0.07	8.3	+/-	0.2	4.1	+/-	0.08		
L69	6.2	+/-	0.1	4.0	+/-	0.05	6.7	+/-	0.1	3.8	+/-	0.05	7.5	+/-	0.1	4.1	+/-	0.05		
V70	7	+/-	0.1	3.9	+/-	0.05	7.5	+/-	0.1	4	+/-	0.05	8.6	+/-	0.1	3.9	+/-	0.05		
L71	7.9	+/-	0.1	4.8	+/-	0.06	9	+/-	0.1	4.6	+/-	0.06	10.3	+/-	0.1	4.4	+/-	0.06		
R72	6	+/-	0.1	3.7	+/-	0.04	6.7	+/-	0.1	3.5	+/-	0.04	7.7	+/-	0.1	3.4	+/-	0.04		
L73																				
R74																				
G75	3.5	+/-	0.1	2.6	+/-	0.03	3.7	+/-	0.1	2.5	+/-	0.03	4	+/-	0.1	2.4	+/-	0.03		
G76	2.7	+/-	0.0	2.2	+/-	0.02	2.5	+/-	0.0	2.1	+/-	0.02	3	+/-	0.0	2.1	+/-	0.02		

References

1. Erlach MB, *et al.* (2016) Pressure dependence of backbone chemical shifts in the model peptides Ac-Gly-Gly-Xxx-Ala-NH2. *J. Biomol. NMR* 65(2):65-77.
2. Maltsev AS, Ying JF, & Bax A (2012) Deuterium isotope shifts for backbone 1H, 15N and 13C nuclei in intrinsically disordered protein alpha-synuclein. *J. Biomol. NMR*. 54:181-191.
3. Nielsen JT & Mulder FAA (2018) POTENCI: prediction of temperature, neighbor and pH-corrected chemical shifts for intrinsically disordered proteins. *J. Biomol. NMR* <https://doi.org/10.1007/s10858-018-0166-5>.
4. Shen Y, Roche J, Grishaev A, & Bax A (2018) Prediction of nearest neighbor effects on backbone torsion angles and NMR scalar coupling constants in disordered proteins. *Protein Sci.* 27(1):146-158.
5. Akasaka K & Li H (2001) Low-lying excited states of proteins revealed from nonlinear pressure shifts in H-1 and N-15 NMR. *Biochemistry* 40(30):8665-8671.
6. Koehler J, *et al.* (2012) Pressure Dependence of N-15 Chemical Shifts in Model Peptides Ac-Gly-Gly-X-Ala-NH2. *Materials* 5(10):1774-1786.